

Stochastic Modeling and Particle Filtering Algorithms for Tracking a Frequency-Hopped Signal

Alexandros Valyrakis, Efthimios E. Tsakonas, Nicholas D. Sidiropoulos, *Fellow, IEEE*, and Ananthram Swami, *Fellow, IEEE*

Abstract—The problem of tracking a frequency-hopped signal without knowledge of its hopping pattern is considered. The problem is of interest in military communications, where, in addition to frequency, hop timing can also be randomly shifted to guard against unauthorized reception and jamming. A conceptually simple nonlinear and non-Gaussian stochastic state-space model is proposed to capture the randomness in carrier frequency and hop timing. This model is well-suited for the application of particle filtering tools: it is possible to compute the optimal (weight variance-minimizing) importance function in closed-form. A convenient mixture representation of the latter is employed together with Rao-Blackwellization to derive a very simple optimal sampling procedure. This is representative of the state-of-art in terms of systematic design of particle filters. A heuristic design approach is also developed, using the mode of the spectrogram to localize hop particles. Performance is assessed in a range of experiments using both simulated and measured data. Interestingly, the results indicate that the heuristic design approach can outperform the systematic one, and both are robust to model assumptions.

Index Terms—Frequency hopping, particle filtering, random hop timing, synchronization, timing jitter, tracking.

I. INTRODUCTION

TRACKING the time-varying parameters (frequency, complex amplitude) of a complex sinusoid is an important problem that arises in numerous applications. In many cases the parameters can be assumed to vary slowly in time; in frequency hopping (FH) communications, however, the carrier frequency is intentionally hopped in a (pseudo-) random and discontinuous fashion. In military communications, FH is used to guard against unauthorized reception and jamming, and hop timing can also be randomized for added protection. In civilian communications (e.g., Bluetooth), FH is used to avoid persistent interference and enable uncoordinated coexistence with other systems.

Manuscript received September 10, 2008; accepted February 14, 2009. First published April 10, 2009; current version published July 15, 2009. The associate editor coordinating the review of this manuscript and approving it for publication was Dr. Zhengyuan (Daniel) Xu. This work was supported in part by the Army Research Laboratory (ARL) through the Collaborative Technology Alliance for Communications and Networks under Cooperative Agreement DADD19-01-2-0011, and in part by ERO Contract N62558-03-C-0012. Preliminary versions of parts of this work were presented at IEEE ICASSP, Toulouse, France, May 15–19, 2006, and in IEEE CAMSAP, St. Thomas, U.S. Virgin Islands, Dec. 12–14, 2007.

A. Valyrakis, E. E. Tsakonas, and N. D. Sidiropoulos are with the Department of Electronic and Computer Engineering, Technical University of Crete, 73100 Chania-Crete, Greece (e-mail: alevali@telecom.tuc.gr; alevali@gmail.com; etsakwnas@gmail.com; nikos@telecom.tuc.gr, nisidiropoulos@gmail.com).

A. Swami is with the Army Research Laboratory, Adelphi, MD 20783 USA (e-mail: a.swami@ieee.org; aswami@arl.army.mil).

Digital Object Identifier 10.1109/TSP.2009.2020765

Several researchers have considered the problem of tracking a FH signal without knowledge of the hopping pattern [2], [3], [9], [10], [13]. Nonparametric methods based on the spectrogram [2], [13] are simple and useful as exploratory tools, but suffer from limited resolution due to leakage. It is possible to employ time-frequency distributions that are better-adapted to frequency hopping [3], but the results are still not very satisfactory. Parametric methods for frequency hopping explicitly model the frequency as piecewise-constant, assume a “budget” on the number of hops within a given observation interval, and employ Dynamic Programming (DP) to track the sought frequency and complex amplitude parameters [9], [10]. Other than an upper bound on the number of hops, the methods in [9], [10] do not assume anything else about the frequencies or complex amplitudes, which are treated as deterministic unknowns. The algorithms in [2], [9], [10], and [13] are also applicable when hop timing is random.

A different viewpoint is adopted in this paper. A stochastic nonlinear, non-Gaussian state-space formulation is proposed, which captures frequency hopping dynamics in a probabilistic sense. The proposed formulation is naturally well-suited for the application of particle filtering for state estimation. Compared to the prior state-of-art in [9] and [10], the new approach has a number of desirable features. For a fixed average hop rate, the complexity of the DP algorithms in [9], [10] is roughly fourth-order polynomial in the number of temporal signal snapshots, T , and DP requires back-tracking—implying that only short data records can be processed, and in batch mode. Particle filtering can be implemented on-line, and its complexity is linear in T . Furthermore, unlike previous methods, the stochastic state-space model can be easily tailored to match a given scenario (e.g., spread bandwidth and modulation).

In closing this section, we remark that particle filtering solutions for tracking *slowly varying* parameters of a harmonic or chirp signal are discussed in [14] and [15]. Interestingly, the case of slowly varying parameters is much different, and in a sense more difficult than the one considered here. In particular, the divergence phenomenon encountered in [14] and [15] is not present in the case of FH.

II. FH DATA MODEL AND PROBLEM STATEMENT

For simplicity of exposition, the case of two receive antennas is discussed in the sequel, but the derivations in the Appendix cover the case of $L \geq 1$ antennas.

Let $\mathbf{x}_k := [\omega_k, A_k, B_k]'$, denote the *state* at time k , where $\omega_k \in [-\pi, \pi)$ denotes instantaneous frequency, $A_k \in \mathbb{C}$ and $B_k \in \mathbb{C}$ denote the complex amplitude of the received signal at the first and second antenna, respectively, and $'$ is used to denote

transposition (to avoid ambiguity with T , which is reserved for the number of temporal snapshots). Let $\mathbf{u}_k := [b_k, \tilde{\omega}_k, \tilde{A}_k, \tilde{B}_k]'$ denote an auxiliary independent and identically distributed (i.i.d.) sequence of vectors with independent components and the following marginal statistics: b_k is a binary random variable with $Pr(b_k = 1) = h$; $\tilde{\omega}_k$ is uniformly distributed over $[-\pi, \pi)$, denoted $\mathcal{U}([-\pi, \pi))$; and \tilde{A}_k and \tilde{B}_k are $\mathcal{CN}(0, 2\sigma_A^2)$, i.e., complex circular Gaussian of total variance $2\sigma_A^2$. The state is assumed to evolve according to the following stochastic model: (see the equations at the bottom of the page) and the scalar measurements at time k are and the scalar measurements at time k are

$$\begin{aligned} y_k(1) &= \mathbf{x}_k(2)e^{j\mathbf{x}_k(1)k} + v_k(1) \\ y_k(2) &= \mathbf{x}_k(3)e^{j\mathbf{x}_k(1)k} + v_k(2) \end{aligned}$$

where $v_k(\cdot)$ denotes i.i.d. $\mathcal{CN}(0, 2\sigma_n^2)$ measurement noise.

Some comments on our modeling assumptions are useful at this point.

- Hops are modeled as random, i.i.d., with hop probability h per sample interval. This is different from traditional models of frequency hopping, which assume that the frequency hops periodically. The random hopping model is i) well-motivated for military communications, ii) well-suited for on-line sequential estimation using particle filtering, and iii) the resulting algorithms can also track periodically hopped signals, as we will see in experiments with measured data.
- When the (discrete-time, baseband-equivalent) frequency hops, it hops anywhere within $[-\pi, \pi)$ with a uniform density. This is appropriate for FH signals sampled at the Nyquist rate relative to the hopping bandwidth.
- Modulation-induced variations can be neglected when the objective is to estimate carrier frequency, but could also be explicitly modeled using, e.g., a smooth autoregressive frequency variation model in-between hops, in lieu of the simplified constant model postulated above.
- We assume i.i.d. Rayleigh fading in space and frequency. This is realistic for frequency-hopped signals in rich multipath environments without a dominant line-of-sight, when the receive antennas are sufficiently well-separated (a few wavelengths apart). Aside from plausibility, this assumption is also convenient for tractability considerations.

Given a sequence of observations $\{\mathbf{y}_k\}_{k=1}^T$, our *objective* is to estimate the sequence of system states $\{\mathbf{x}_k\}_{k=1}^T$ —that is, the unknown carrier frequencies and complex amplitudes. We will do this in an indirect way—estimating the posterior density $p(\mathbf{x}_k | \{\mathbf{y}_l\}_{l=1}^k)$, from which the state can be estimated using the conditional mean. This leads us to particle filtering.

The rest of the paper is organized as follows. Section III is a very brief review of the basic elements of particle filtering.

A custom particle filtering solution for random time-frequency hopping is derived in Section IV. This includes the computation of the optimal importance function in closed-form. A key idea is to employ a convenient mixture representation of the optimal importance function, which enables use of Rao-Blackwellization. This solution is representative of the state-of-art in terms of *systematic* design of particle filters. An alternative heuristic design is developed in Section V. Results of experiments with simulated and measured FH data are presented in Section VI, and conclusions are drawn in Section VII.

III. PARTICLE FILTERING (PF)

PF is an important estimation methodology that is applicable to general stochastic nonlinear and/or non-Gaussian state-space models. We refer the reader to [1], [4], and [7] for recent tutorial overviews of PF. In PF, a continuous distribution $p(\mathbf{x})$ is approximated by a discrete random measure comprising “particles” (locations \mathbf{x}_n) and corresponding weights w_n

$$p(\mathbf{x}) \approx \sum_{n=1}^N w_n \delta(\mathbf{x} - \mathbf{x}_n)$$

where $\delta(\cdot)$ denotes the Dirac delta function. If our goal is to estimate the system state at time k from measurements up to and including time k , the key distribution of interest is the posterior density $p(\mathbf{x}_k | \{\mathbf{y}_l\}_{l=1}^k)$. PF starts with a random measure approximation of the initial state distribution, and uses subsequent measurements to estimate $p(\mathbf{x}_k | \{\mathbf{y}_l\}_{l=1}^k)$, $k \in \{1, 2, \dots\}$ in a sequential fashion, i.e., generate a sequence of random measure approximations

$$\hat{p}(\mathbf{x}_k | \{\mathbf{y}_l\}_{l=1}^k) = \sum_{n=1}^N w_{n,k} \delta(\mathbf{x}_k - \mathbf{x}_{n,k}).$$

Direct sampling from the desired posterior is not possible in most cases. For this reason, we resort to *importance sampling*: we draw samples from a suitable *importance function* that has the same support as the desired posterior, and we weigh the particles according to the ratio of the two densities at the sample point. The choice of importance function is key—the more it resembles the desired density the better, but it should also facilitate easy sampling.

A common problem in PF is *degeneracy*: the weights of all except a few particles become negligible after several iterations. This can be detected and corrected using *resampling* techniques [1], [4], [7]. The importance function that minimizes the variance of the weights (a precaution against degeneracy) is

$$p(\mathbf{x}_k | \mathbf{x}_{n,k-1}, \mathbf{y}_k) = \frac{p(\mathbf{y}_k | \mathbf{x}_k) p(\mathbf{x}_k | \mathbf{x}_{n,k-1})}{\int_{\mathbf{x}} p(\mathbf{y}_k | \mathbf{x}) p(\mathbf{x} | \mathbf{x}_{n,k-1}) d\mathbf{x}}.$$

$$\begin{aligned} \mathbf{x}_k &= f(\mathbf{x}_{k-1}, \mathbf{u}_k) \\ &= \begin{cases} \mathbf{x}_{k-1}, & \mathbf{u}_k(1) = 0 \\ [\mathbf{u}_k(2), \mathbf{u}_k(3), \mathbf{u}_k(4)]', & \mathbf{u}_k(1) = 1 \end{cases} \\ &= \begin{cases} \mathbf{x}_{k-1}, & w.p. 1 - h \\ [\mathcal{U}([-\pi, \pi)), \mathcal{CN}(0, 2\sigma_A^2), \mathcal{CN}(0, 2\sigma_A^2)]', & w.p. h \end{cases} \end{aligned}$$

This is often referred to as the *optimal importance function*, and it usually strikes a better estimation performance-complexity trade-off than other alternatives. Notice that the optimal importance function takes into account the latest measurement. Both the prior and the optimal importance function yield consistent estimates of the desired density as the number of particles goes to infinity.

There are two obstacles to using the optimal importance function: it requires integration to compute the normalization factor (which is usually intractable); and sampling from it can be complicated. Thankfully, it turns out that both obstacles can be overcome for our particular model, as shown next.

IV. CLOSED-FORM OPTIMAL IMPORTANCE FUNCTION AND SAMPLING PROCEDURE FOR RANDOM FREQUENCY HOPPING

Denote $\mathbf{x}_k := [\omega_k, A_k, B_k]'$, where $\omega_k \in [-\pi, \pi)$, and $A_k, B_k \in \mathbb{C}$; and likewise $\mathbf{x}_{n,k-1} := [\omega_{n,k-1}, A_{n,k-1}, B_{n,k-1}]'$. Let $\mathbf{x} := [\omega, A, B]'$, and

$$D(\mathbf{y}_k, \mathbf{x}_{n,k-1}) := \int_{\mathbf{x}} p(\mathbf{y}_k | \mathbf{x}) p(\mathbf{x} | \mathbf{x}_{n,k-1}) d\mathbf{x}.$$

Then

$$\begin{aligned} D(\mathbf{y}_k, \mathbf{x}_{n,k-1}) &= \int_{\omega \in [-\pi, \pi)} \int_{A \in \mathbb{C}} \int_{B \in \mathbb{C}} \frac{1}{2\pi\sigma_n^2} \\ &\times e^{-\frac{|\mathbf{y}_k(1) - A e^{j\omega k}|^2}{2\sigma_n^2}} \frac{1}{2\pi\sigma_n^2} e^{-\frac{|\mathbf{y}_k(2) - B e^{j\omega k}|^2}{2\sigma_n^2}} \\ &\times \left[(1-h)\delta(\omega - \omega_{n,k-1}) \right. \\ &\times \delta(A - A_{n,k-1})\delta(B - B_{n,k-1}) \\ &\left. + \frac{h}{2\pi} \frac{1}{2\pi\sigma_A^2} \frac{1}{2\pi\sigma_A^2} e^{-\frac{|A|^2}{2\sigma_A^2}} e^{-\frac{|B|^2}{2\sigma_A^2}} \right] dA dB d\omega. \end{aligned}$$

This integral can be computed by completing the squares, yielding the top equation shown at the bottom of the page. The weight update for the optimal importance function is

$$w_{n,k} \propto w_{n,k-1} p(\mathbf{y}_k | \mathbf{x}_{n,k-1}) = w_{n,k-1} D(\mathbf{y}_k, \mathbf{x}_{n,k-1})$$

followed by normalization to 1. We need a way to sample from the optimal importance function. As a first step towards this end, note that $p(\mathbf{x}_k | \mathbf{x}_{n,k-1}, \mathbf{y}_k)$ can be written as a mixture of two pdfs

$$p(\mathbf{x}_k | \mathbf{x}_{n,k-1}, \mathbf{y}_k) = (1 - \tilde{h}) p_0(\mathbf{x}_k | \mathbf{x}_{n,k-1}, \mathbf{y}_k) + \tilde{h} p_1(\mathbf{x}_k | \mathbf{x}_{n,k-1}, \mathbf{y}_k)$$

where the constituent pdfs and the *posterior hop rate* \tilde{h} are shown at the bottom of the page. It follows that with probability $1 - \tilde{h}$ we simply copy the previous particle, else we draw a particle from $p_1(\mathbf{x}_k | \mathbf{x}_{n,k-1}, \mathbf{y}_k)$. For the latter step, we will construct a technique based on Rao-Blackwellization (see [5], [6], [11], and references therein). Although this is presented here for the case of two receive antennas, it is straightforward to generalize to L receive antennas. The pdf $p_1(\mathbf{x}_k | \mathbf{x}_{n,k-1}, \mathbf{y}_k)$ can be factored as

$$p_1(\mathbf{x}_k | \mathbf{x}_{n,k-1}, \mathbf{y}_k) = p(A_k, B_k | \omega_k, \mathbf{x}_{n,k-1}, \mathbf{y}_k) p(\omega_k | \mathbf{x}_{n,k-1}, \mathbf{y}_k).$$

Since we already know analytically $p_1(\mathbf{x}_k | \mathbf{x}_{n,k-1}, \mathbf{y}_k)$ we can derive $p(\omega_k | \mathbf{x}_{n,k-1}, \mathbf{y}_k)$ by direct integration

$$\begin{aligned} p(\omega_k | \mathbf{x}_{n,k-1}, \mathbf{y}_k) &= \int_{A_k \in \mathbb{C}} \int_{B_k \in \mathbb{C}} p_1(\omega_k, A_k, B_k | \mathbf{x}_{n,k-1}, \mathbf{y}_k) dA_k dB_k \\ &= \frac{2\pi (\sigma_A^2 + \sigma_n^2)^2}{(2\pi\sigma_A^2)^2 (2\pi\sigma_n^2)^2} \int_{A_k \in \mathbb{C}} e^{-\frac{|\mathbf{y}_k(1) - A_k e^{j\omega k}|^2}{2\sigma_n^2}} \\ &\times e^{-\frac{|A_k|^2}{2\sigma_A^2}} dA_k \\ &\times \int_{B_k \in \mathbb{C}} e^{-\frac{|\mathbf{y}_k(2) - B_k e^{j\omega k}|^2}{2\sigma_n^2}} e^{-\frac{|B_k|^2}{2\sigma_A^2}} dB_k. \end{aligned}$$

$$D(\mathbf{y}_k, \mathbf{x}_{n,k-1}) = \frac{h}{(2\pi)^2 (\sigma_n^2 + \sigma_A^2)^2} e^{-\frac{|\mathbf{y}_k(1)|^2 + |\mathbf{y}_k(2)|^2}{2(\sigma_n^2 + \sigma_A^2)}} + \frac{1-h}{(2\pi\sigma_n^2)^2} e^{-\frac{|\mathbf{y}_k(1) - A_{n,k-1} e^{j\omega_{n,k-1} k}|^2}{2\sigma_n^2} - \frac{|\mathbf{y}_k(2) - B_{n,k-1} e^{j\omega_{n,k-1} k}|^2}{2\sigma_n^2}}.$$

$$\begin{aligned} p_0(\mathbf{x}_k | \mathbf{x}_{n,k-1}, \mathbf{y}_k) &:= \delta(\omega_k - \omega_{n,k-1}) \delta(A_k - A_{n,k-1}) \delta(B_k - B_{n,k-1}), \\ p_1(\mathbf{x}_k | \mathbf{x}_{n,k-1}, \mathbf{y}_k) &:= \frac{\frac{1}{(2\pi)^5} \frac{1}{(\sigma_A^2 \sigma_n^2)^2} e^{-\frac{|\mathbf{y}_k(1) - A_k e^{j\omega k}|^2}{2\sigma_n^2} - \frac{|\mathbf{y}_k(2) - B_k e^{j\omega k}|^2}{2\sigma_n^2} - \frac{|A_k|^2 + |B_k|^2}{2\sigma_A^2}}}{\frac{1}{(2\pi)^2} \frac{1}{(\sigma_n^2 + \sigma_A^2)^2} e^{-\frac{|\mathbf{y}_k(1)|^2 + |\mathbf{y}_k(2)|^2}{2(\sigma_n^2 + \sigma_A^2)}}}, \end{aligned}$$

and

$$\tilde{h} := h \frac{\frac{1}{(2\pi)^2} \frac{1}{(\sigma_n^2 + \sigma_A^2)^2} e^{-\frac{|\mathbf{y}_k(1)|^2 + |\mathbf{y}_k(2)|^2}{2(\sigma_n^2 + \sigma_A^2)}}}{D(\mathbf{y}_k, \mathbf{x}_{n,k-1})}$$

By completing the squares in each of the two integrals above, we come up with the analytical form of the desired pdf

$$p(\omega_k | \mathbf{x}_{n,k-1}, \mathbf{y}_k) = \frac{1}{2\pi}.$$

It is interesting that this density does not depend on the measurement \mathbf{y}_k —the information provided by the measurement at time k is totally absorbed in the posterior hop rate \tilde{h} .

Next, we derive an analytical formula for $p(A_k, B_k | \omega_k, \mathbf{x}_{n,k-1}, \mathbf{y}_k)$. Using the factorization above and the result for $p(\omega_k | \mathbf{x}_{n,k-1}, \mathbf{y}_k)$, we have the first equation at the bottom of the page. Upon defining $\sigma^2 := (\sigma_A^2 \sigma_n^2) / (\sigma_A^2 + \sigma_n^2)$, $W_A := (\sigma_A^2 \mathbf{y}_k(1) e^{-j\omega_k k}) / (\sigma_A^2 + \sigma_n^2)$, $W_B := (\sigma_n^2 \mathbf{y}_k(2) e^{-j\omega_k k}) / (\sigma_A^2 + \sigma_n^2)$, and after straightforward manipulations, $p(A_k, B_k | \omega_k, \mathbf{x}_{n,k-1}, \mathbf{y}_k)$ can be written as

$$p(A_k, B_k | \omega_k, \mathbf{x}_{n,k-1}, \mathbf{y}_k) = \frac{1}{2\pi\sigma^2} e^{-\frac{|A_k - W_A|^2}{2\sigma^2}} \frac{1}{2\pi\sigma^2} e^{-\frac{|B_k - W_B|^2}{2\sigma^2}}.$$

This form of $p(A_k, B_k | \omega_k, \mathbf{x}_{n,k-1}, \mathbf{y}_k)$ along with the factorization of $p_1(\mathbf{x}_k | \mathbf{x}_{n,k-1}, \mathbf{y}_k)$ enables us to easily sample the optimal importance density. Sampling can be carried out by first drawing a frequency sample from $\mathcal{U}([- \pi, \pi])$ and then using it to draw a sample from $p(A_k, B_k | \omega_k, \mathbf{x}_{n,k-1}, \mathbf{y}_k)$, which is a simple Gaussian density.

Remark: Notice that, due to the use of the equivalent mixture representation (involving the posterior hop rate) and the fact that Rao-Blackwellization is only applied to draw hop particles, no Kalman filtering is needed here, in contrast with [5], [6], [11], and [15]. This saves a lot of computations.

V. AUXILIARY SPECTROGRAM PARTICLE FILTERING (ASPECT-PF)

The use of the optimal (weight variance-minimizing) importance function coupled with Rao-Blackwellization is representative of the state-of-art in terms of systematic design of particle filters. Note, however, that the ultimate objective is a favorable balance of estimation (tracking) accuracy and complexity. Minimizing the variance of the weights often strikes a better accuracy-complexity trade-off than other particle filtering solutions, but this is not guaranteed.

The key open problem in particle filtering is the choice of importance function. Custom solutions may outperform systematic ones by insightful design of the importance function. This is presently more a matter of engineering art, rather than theory.

Consider using a short-window spectrogram estimator of the instantaneous frequency, and two adjacent dwells. So long as the spectrogram window is contained within a single dwell, its mode will be a good estimate of the corresponding carrier frequency. Transient effects come into play as the window crosses the hop between the two dwells, and then the mode catches up with the new carrier frequency. The idea is to draw from a narrow interval about the mode of the spectrogram with probability h , else copy the previous particle. As the window begins crossing a hop, new particles are drawn around the forthcoming carrier frequency; yet these particles are inconsistent with the present measurement. If $p(y_k | \mathbf{x}_{n,k})$ is used to weigh the particles, new particles will be down-weighted relative to old particles. The situation reverses as the window crosses the hop: old particles are down-weighted relative to new particles.

Let $\hat{\omega}_k$ denote the mode of the spectrogram at time k , based on a causal window from $y_{k-\ell+1}$ to y_k . The proposed function employed by *auxiliary spectrogram PF* (ASPECT-PF) is¹

$$(1-h)\delta(\omega_k - \omega_{n,k-1})\delta(A_k - A_{n,k-1}) + hp(\omega_k) \frac{1}{2\pi\sigma_A^2} e^{-\frac{|A_k|^2}{2\sigma_A^2}}$$

with $p(\omega_k)$ defined as

$$p(\omega_k) := \frac{1}{\sqrt{2\pi}\sigma_S} e^{-\frac{(\omega_k - \hat{\omega}_k)^2}{2\sigma_S^2}}$$

with σ_S small (10^{-3} in our experiments).

For this choice of importance distribution, the particle weight update is given by the second equation at the bottom of the page. If $\omega_{n,k} \neq \omega_{n,k-1}$ and $A_{n,k} \neq A_{n,k-1}$, then

$$w_{n,k} \propto w_{n,k-1} \frac{\sigma_S}{\sqrt{2\pi}} \exp\left(\frac{(\omega_{n,k} - \hat{\omega}_k)^2}{2\sigma_S^2}\right) p(y_k | \mathbf{x}_{n,k})$$

else the weight update becomes indefinite due to the Dirac deltas, and we use

$$w_{n,k} \propto w_{n,k-1} \frac{\sigma_S}{\sqrt{2\pi}} p(y_k | \mathbf{x}_{n,k}).$$

¹We only consider the single-channel case for brevity.

$$p(A_k, B_k | \omega_k, \mathbf{x}_{n,k-1}, \mathbf{y}_k) = \frac{\frac{1}{(2\pi\sigma_A)^2} \frac{1}{(2\pi\sigma_n)^2} e^{-\frac{|\mathbf{y}_k(1) - A_k e^{j\omega_k k}|^2}{2\sigma_n^2}} e^{-\frac{|A_k|^2}{2\sigma_A^2}} e^{-\frac{|\mathbf{y}_k(2) - B_k e^{j\omega_k k}|^2}{2\sigma_n^2}} e^{-\frac{|B_k|^2}{2\sigma_A^2}}}{\frac{1}{(2\pi)^2} \frac{1}{(\sigma_n^2 + \sigma_A^2)^2} e^{-\frac{|\mathbf{y}_k(1)|^2 + |\mathbf{y}_k(2)|^2}{2(\sigma_n^2 + \sigma_A^2)}}}.$$

$$w_{n,k} \propto w_{n,k-1} p(y_k | \mathbf{x}_{n,k}) \left[\frac{(1-h)\delta(\omega_{n,k} - \omega_{n,k-1})\delta(A_{n,k} - A_{n,k-1}) + \frac{h}{2\pi} \frac{1}{2\pi\sigma_A^2} e^{-\frac{|A_{n,k}|^2}{2\sigma_A^2}}}{(1-h)\delta(\omega_{n,k} - \omega_{n,k-1})\delta(A_{n,k} - A_{n,k-1}) + hp(\omega_{n,k}) \frac{1}{2\pi\sigma_A^2} e^{-\frac{|A_{n,k}|^2}{2\sigma_A^2}}} \right].$$

Performance can be further improved by using a short look-ahead (noncausal) window, i.e., $\hat{\omega}_k$ computed from y_k to $y_{k+\ell-1}$. This is often tolerable in applications for small ℓ .

VI. EXPERIMENTS

In our experiments, we compared the following PF algorithms:

- SIR: the standard Sampling Importance Resampling algorithm using the prior importance function [1].
- OIF-RBPF: using the Optimal Importance Function (OIF) and Rao-Blackwellization.
- ASPECT-PF-C: the Causal (C) version, with spectrogram window length $\ell = 4$ or $\ell = 8$, zero-padding to 256 samples, and $\sigma_S = 10^{-3}$.
- ASPECT-PF-NC: the Non-Causal (NC) version, with window length $\ell = 8$ or $\ell = 16$ and otherwise the same choice of parameters.

For the PF algorithms, the initial state was assumed known. This is reasonable for tracking applications, following initial acquisition. In all cases, we used resampling at each time step—in particular, the *multinomial* resampling [8] implementation of Arnaud Doucet and Nando de Freitas. We used root mean square error (RMSE) of frequency estimation as a performance measure.

We also included a simple spectrogram estimator (SpE) as a baseline. For each time instant k , SpE computes the periodogram of $\{y_{k-\ell+1}, \dots, y_k\}$ in the causal case or $\{y_k, \dots, y_{k+\ell-1}\}$ in the noncausal case, and then finds its mode. Zero-padding to 256 samples was used for SpE, as for ASPECT-PF. Unlike ASPECT-PF, the causal and noncausal versions of SpE have the same performance—the noncausal version is equivalent to running the causal version backwards in time (time-reversal)².

SpE can be efficiently implemented by peak-picking a full-overlap factor rectangularly-windowed spectrogram, requires minimal parameter tuning (choice of window length, ℓ , which was manually optimized in our experiments), and is the first exploratory method that one would use in practice.

We conducted experiments with simulated and measured data:

- The simulated data were generated using our model, and the PF algorithms utilized the correct model parameters. This is meant to assess the performance potential of the proposed algorithms under controlled conditions.
- We also conducted experiments using measured data which deviate significantly from our modeling assumptions.

The specific setups and associated results are presented next.

A. Simulations

For the simulated data, we used $\sigma_A^2 = 1$, and $\sigma_n^2 = 0.1$ to generate data and as model parameters for the PF algorithms for all cases considered.

1) *Single-Channel Case*: Fig. 1 shows RMSE results for the aforementioned single-channel PF algorithms, for $T = 100$ and $h = 0.01$, as a function of the number of particles. The performance of SpE is a constant, given in the caption for clarity. The

²This argument does not apply to tracking filters like ASPECT-PF which have built-in *memory*.

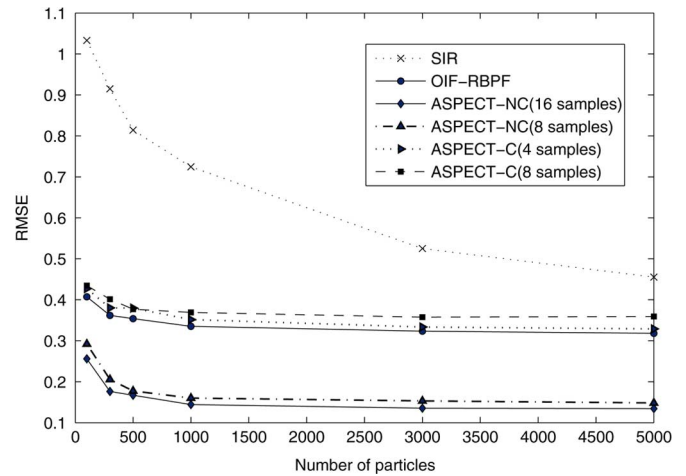


Fig. 1. Single-channel RMSE results for $T = 100$, $h = 0.01$, and 800 MC trials. As a baseline, the spectrogram estimator (SpE) with optimized window length (8) yields an RMSE of 0.4.

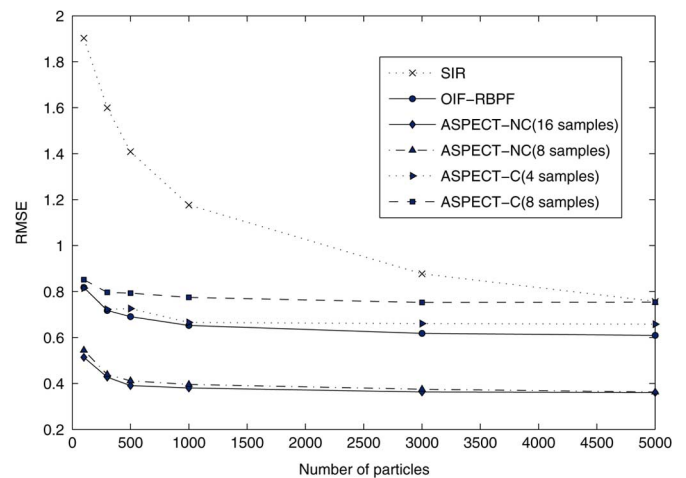


Fig. 2. Single-channel RMSE results for $T = 300$, $h = 0.02$, and 500 MC trials. The spectrogram estimator (SpE) with optimized window length (8) yields an RMSE of 0.82.

results are averaged over 800 Monte Carlo (MC) trials. Fig. 2 shows corresponding results for $T = 300$, $h = 0.02$, and 500 MC trials, and otherwise the same setup as in Fig. 1.

The SIR is simple to derive and implement, however Figs. 1 and 2 show that its RMSE performance leaves much to be desired. OIF-RBPF is the best causal filter, but ASPECT-PF-C is not far from it. The comparison of ASPECT-PF-NC to the causal filters is of course not on equal footing; still, it is interesting to see the kind of improvement possible when one can afford a little delay.

In order to get a feel for the tracking capabilities of the different filters, Fig. 3 shows typical tracks for OIF-RBPF, ASPECT-PF-C (window length 4), and ASPECT-PF-NC (window length 8), for $T = 500$, $h = 0.01$, and 1000 particles for each filter.

Tracking performance also depends on system parameters, notably the measurement noise variance and the frequency hopping probability. In order to illustrate this dependence, Fig. 4 shows RMSE for the various PF algorithms as a function of measurement noise variance for $T = 100$, $h = 0.01$, $N = 1000$, and 500 MC trials. Likewise, Fig. 5 shows

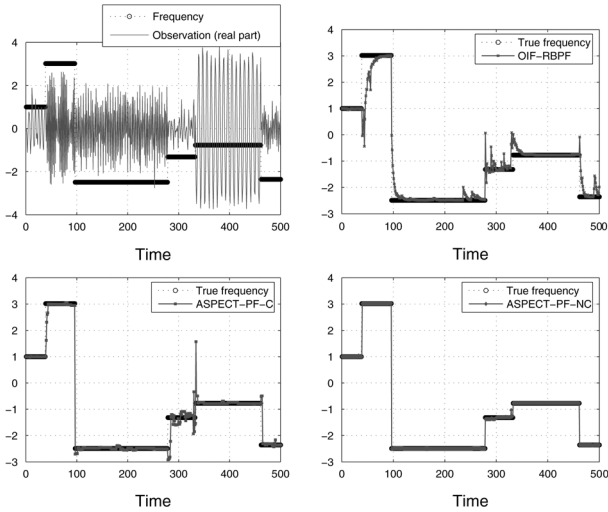


Fig. 3. Illustration of typical tracking performance for 1000 particles, $T = 500$, $h = 0.01$.

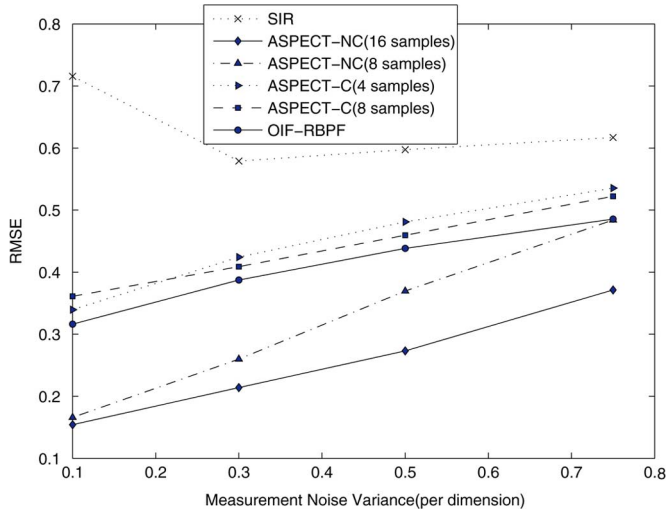


Fig. 4. RMSE comparison of PF algorithms as a function of measurement noise variance for $T = 100$, $h = 0.01$, $N = 1000$, and 500 MC trials.

RMSE as a function of frequency hopping probability, h , for $T = 100$, $N = 1000$, $\sigma_n^2 = 0.1$ and 500 MC trials. Naturally, performance degrades with increasing noise variance or frequency hopping probability (in the latter case there are less samples to estimate the frequency of each dwell). In Fig. 4, observe that ASPECT-PF-C with an 8-sample window performs better than ASPECT-PF-C with a 4-sample window when the measurement noise variance is 0.25 or more, due to better noise averaging. The situation is reversed for measurement noise variance under 0.25. In the same figure, the SIR filter yields poor performance when the measurement noise variance is low - this can be attributed to a higher sensitivity with respect to degeneracy, stemming from the use of a relatively naive (the prior) importance function. In Fig. 5, observe that ASPECT-PF-NC with an 8-sample window gives lower RMSE than ASPECT-PF-NC with a 16-sample window as the frequency hopping probability increases. The reason is that very short dwells become more likely in this case.

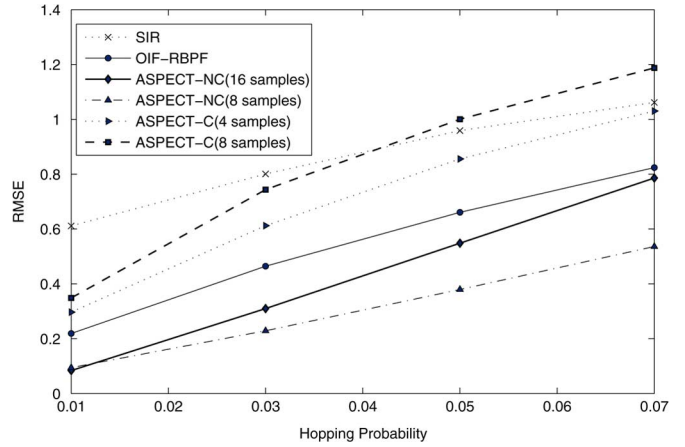


Fig. 5. RMSE comparison of PF algorithms as a function of frequency hopping probability, h , for $T = 100$, $N = 1000$, and 500 MC trials.

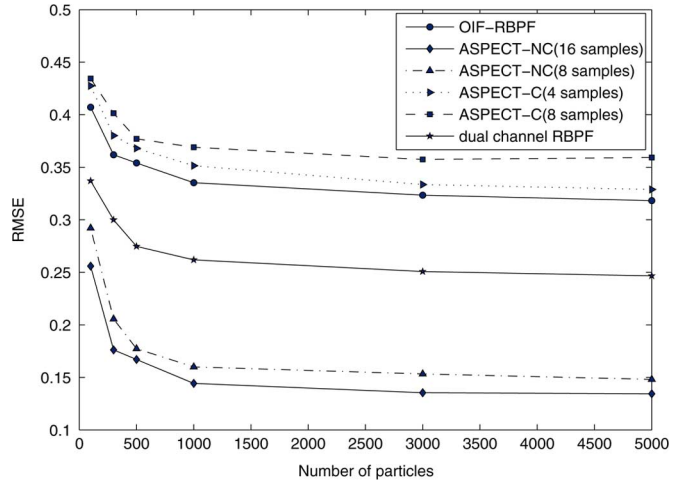


Fig. 6. RMSE comparison of single vs. dual channel PF for $T = 100$, $h = 0.01$, and 500 MC trials.

2) *Dual-Channel Case*: Fig. 6 shows the RMSE performance improvement afforded by dual-channel OIF-RBPF relative to its single-channel version as well as the other single-channel filters. As expected, the dual-channel filter yields significant performance improvement relative to its single-channel counterpart; but single-channel ASPECT-PF-NC is still considerably better. This means that a second antenna and down-conversion chain are not justified when one can afford a little delay.

3) *Complexity*: The complexity of all PF solutions considered is linear in the number of particles, and quantitatively very similar—about 30–40 ms per measurement for a plain-vanilla interpreted Matlab implementation on a typical PC with 1000 particles. The sampling step of all algorithms can be parallelized, and ASPECT-PF-NC yields very good performance with about 250 particles. This makes it an appealing candidate for practical implementation.

B. Measured Data

We further tested our algorithms using measured FH data, made available by Telcordia Technologies through the ARL Collaborative Technology Alliance (ARL-CTA) for Communications and Networks under Cooperative Agreement

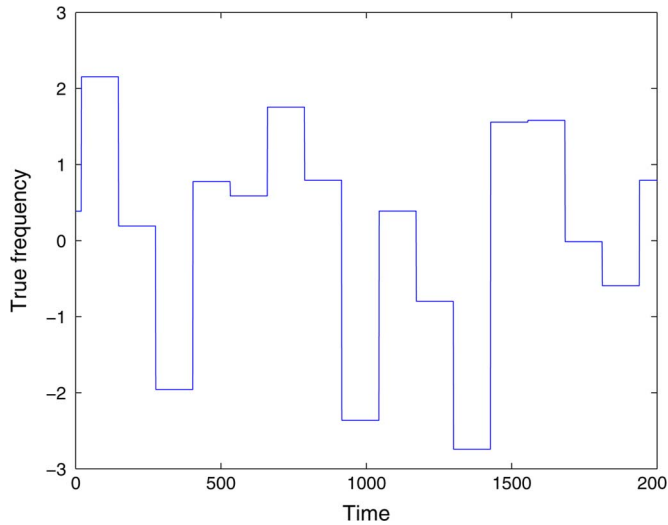


Fig. 7. Hopping sequence for the measured data ($T = 2000$ temporal samples).

DADD19-01-2-0011. The measurement campaign was conducted in 2004, and comprised a diverse array of scenarios. The particular data that we used corresponds to a line-of-sight (LoS) scenario called *T3-LoS*. Over-the-air testing was performed using a software-defined radio and Agilent 4438 synthesizers; the carrier frequency was 1.875 GHz, with a two-sided bandwidth of 1.25 MHz; the signal bandwidth was 1 MHz. The received signal was sampled at 4 Ms/s with a 12-bit ADC. The (baseband) hopping bandwidth was from -0.5 to 0.5 MHz, divided into 32 equispaced frequency bins, and slow FH with binary Gaussian Minimum Shift Keying (GMSK) modulation was used. The maximum modulation-induced frequency deviation was $(1/128)$ -th of the FH bin width.

The transmitted waveform was known, and included a long synchronization preamble, which also affords accurate channel estimation. The received signal was downconverted and oversampled at the receiver by a factor of 4. This compresses the frequency variation to a quarter of the band, and is (grossly) inconsistent with our model; we therefore subsampled the signal prior to processing by a factor of 4. The end result is a full-band SFH GMSK signal with 128 samples per dwell, from which we extracted a segment comprising 2000 samples. The corresponding hopping sequence is plotted in Fig. 7.

There are many reasons why testing with measured data is important. The measured data violate several of our assumptions, which is to be expected in practice:

- Due to the presence of a strong LoS component and only minor multipath, the signal's amplitude is approximately constant across dwells. This violates our i.i.d. Rayleigh fading assumption from dwell to dwell.
- Within a dwell, the frequency is not constant; it varies slowly due to GMSK modulation. This induces a time-varying residual phase noise relative to the true carrier. This is illustrated in Fig. 8, which shows one dwell of the unmodulated and the received signal after downconversion to the hopping bandwidth, synchronization, amplitude, and phase correction. The net effect is that the compound noise term is correlated and non-Gaussian. This is illustrated in

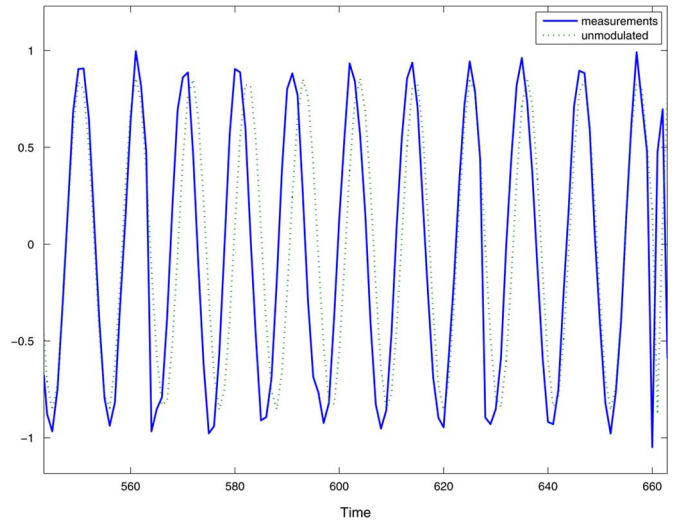


Fig. 8. One dwell of the carrier and the received signal after synchronization, amplitude and phase correction. Notice the residual phase noise due to modulation.

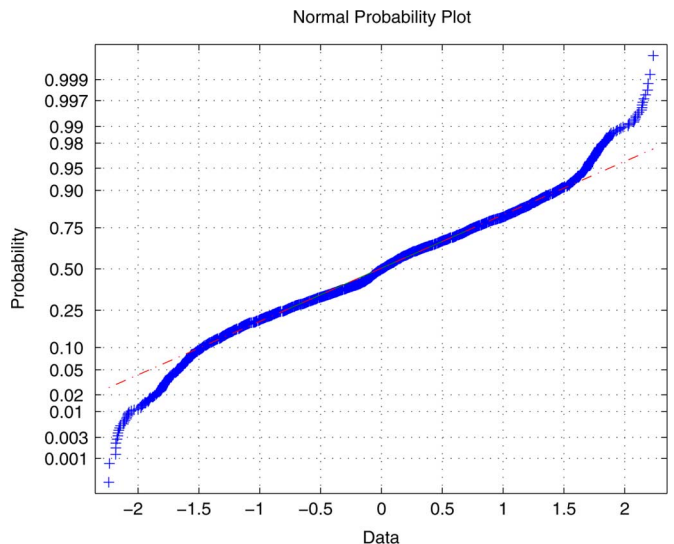


Fig. 9. Normal probability plot of real part of residual signal for $T = 2000$ time steps. Notice significant deviation from Normal distribution in the tails, primarily due to carrier modulation.

Fig. 9, which shows a Normal probability plot of the real part of the noise signal. Notice the significant deviation from the Normal distribution in the tails.

- Carrier hopping is not i.i.d. random as postulated in our model; it is periodic (without intentional jitter—see Fig. 7).
- The parameters of our model ($h, \sigma_A^2, \sigma_n^2$) have to be estimated.

For the above reasons, trying our algorithms on the measured data is a meaningful test of robustness to model mismatch.

The hop period (dwell duration) T_d can be accurately estimated from the spectrogram, or using cyclostationarity. We therefore set $h = 1/T_d = 1/128$. Given T_d , it is possible to segment the signal in fixed-length dwells using a serial acquisition search, and estimate the remaining parameters from the segments. We used $\sigma_A^2 = 1$ (to match the signal power), and $\sigma_n^2 = 0.1$.

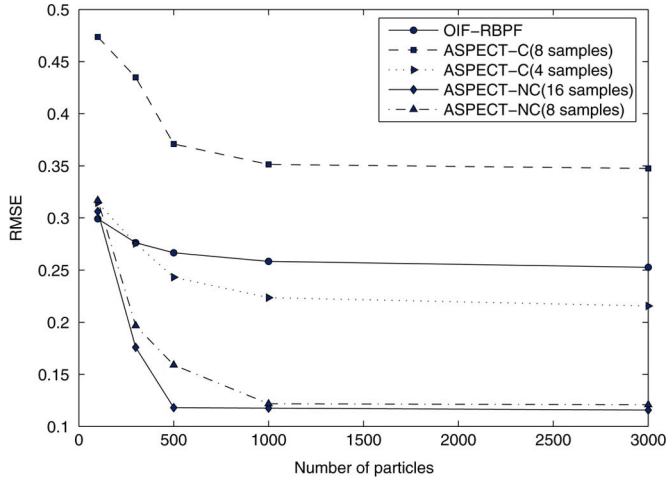


Fig. 10. RMSE results for the measured data: $T = 2000, h = 1/128$. The spectrogram estimator (SpE) with optimized window length (8) yields an RMSE of 0.32.

The results of our experiments using measured data are summarized in Fig. 10. Notice that ASPECT-PF-C with a window length of 4 samples outperforms OIF-RBPF in this model-mismatched case. ASPECT-PF-NC delivers excellent performance with as few as a few hundred particles. To appreciate this, consider the following back-of-the-envelope calculation. If a tracking algorithm misses a half-band hop of π rads by a single sample, but otherwise tracks the signal perfectly over a dwell of 128 samples, the associated RMSE will be approximately 0.27. Most hops are less than half-band, yielding lower RMSE in the same scenario; but there will also be errors over the duration of the dwell. This speaks for a key strength of PF solutions versus window-based methods (such as SpE): the ability to accurately track hop timing.

VII. CONCLUSION

We have considered the problem of tracking a frequency-hopped signal of random dwell frequency and hop timing. Starting from a simple stochastic state-space model, we computed the optimal (weight variance-minimizing) importance function in closed-form. This form is not directly amenable to Rao-Blackwellization; however we proposed a mixture representation that decouples the problem and yields a very simple sampling procedure (OIF-RBPF). A heuristic design (ASPECT-PF) was also developed, using the mode of the spectrogram to localize hop particles. Robustness with respect to model mismatch has been assessed using measured FH data,

which violate many of our assumptions. The measured data feature strong LoS (approximately constant signal amplitude), dwell frequency modulation, periodic hop timing, and correlated non-Gaussian noise—thus significantly departing from our working assumptions. Still, the proposed filters work well, with only a few hundred particles.

APPENDIX I

A. Derivation of Closed Form Expression for the Optimal Importance Density

Assume that L antennas and corresponding receive chains are available, for any $L \geq 1$. The state at time k is $\mathbf{x}_k := [\omega_k, A_k^{(1)}, \dots, A_k^{(L)}]'$ where $\omega_k \in [-\pi, \pi)$ denotes instantaneous frequency and $A_k^{(1)}, \dots, A_k^{(L)} \in \mathbb{C}$ are complex amplitudes. Define the auxiliary i.i.d. sequence of random vectors $\mathbf{u}_k := [b_k, \tilde{\omega}_k, \tilde{A}_k^{(1)}, \dots, \tilde{A}_k^{(L)}]'$, where b_k is a binary random variable with $Pr(b_k = 1) = h$; $\tilde{\omega}_k$ is $\mathcal{U}([-\pi, \pi))$; and $\tilde{A}_k^{(1)}, \dots, \tilde{A}_k^{(L)}$ are i.i.d. $\mathcal{CN}(0, \sigma_A^2)$.

Then (see the equation at the bottom of the page), where $v_k(l)$ denotes $\mathcal{CN}(0, 2\sigma_n^2)$ measurement noise that is assumed to be i.i.d. in space (l) and time (k).

The weight variance-minimizing importance function is [1], [4]

$$p(\mathbf{x}_k | \mathbf{x}_{n,k-1}, \mathbf{y}_k) = \frac{p(\mathbf{y}_k | \mathbf{x}_k)p(\mathbf{x}_k | \mathbf{x}_{n,k-1})}{\int_{\mathbf{x}} p(\mathbf{y}_k | \mathbf{x})p(\mathbf{x} | \mathbf{x}_{n,k-1})d\mathbf{x}}.$$

The integral $D(\mathbf{y}_k, \mathbf{x}_{n,k-1}) := \int_{\mathbf{x}} p(\mathbf{y}_k | \mathbf{x})p(\mathbf{x} | \mathbf{x}_{n,k-1})d\mathbf{x}$ can be computed as follows:

$$\begin{aligned} D(\mathbf{y}_k, \mathbf{x}_{n,k-1}) &= \int_{\omega \in [-\pi, \pi)} \int_{A^{(1)} \in \mathbb{C}} \cdots \int_{A^{(L)} \in \mathbb{C}} \prod_{m=1}^L \left[\frac{1}{2\pi\sigma_n^2} \right. \\ &\quad \times \left. e^{-\frac{|\mathbf{y}_k^{(m)} - A^{(m)} e^{j\omega k}|^2}{2\sigma_n^2}} \right] \\ &\quad \times \left[(1-h)\delta(\omega - \omega_{n,k-1}) \right. \\ &\quad \times \prod_{m=1}^L \delta(A^{(m)} - A_{n,k-1}^{(m)}) \\ &\quad \left. + \frac{h}{2\pi} \prod_{m=1}^L \left(\frac{1}{2\pi\sigma_A^2} e^{-\frac{|A^{(m)}|^2}{2\sigma_A^2}} \right) \right] dA^{(1)} \dots \\ &\quad dA^{(L)} d\omega = D_1 + D_2 \end{aligned}$$

$$\begin{aligned} \mathbf{x}_k &= f(\mathbf{x}_{k-1}, \mathbf{u}_k) \\ &= \begin{cases} \mathbf{x}_{k-1}, & \mathbf{u}_k(1) = 0 \\ [\mathbf{u}_k(2), \dots, \mathbf{u}_k(L+1)]', & \mathbf{u}_k(1) = 1 \end{cases} \\ &= \begin{cases} \mathbf{x}_{k-1}, & w.p. 1-h \\ [\mathcal{U}([-\pi, \pi)), \mathcal{CN}(0, \sigma_A^2), \dots, \mathcal{CN}(0, \sigma_A^2)]', & w.p. h \end{cases} \\ \mathbf{y}_k(l) &= \mathbf{x}_k(l+1)e^{j\mathbf{x}_k(1)k} + v_k(l), \quad l \in \{1, \dots, L\} \end{aligned}$$

where D_1 and D_2 are given at the bottom of the page. The integral inside the brackets in the equation for D_2 can be computed by completing the squares

$$\begin{aligned} \mathfrak{J}_{A(m)} &= \int_{A(m) \in \mathbb{C}} e^{-\frac{|\mathbf{y}_k(m) - A(m)e^{j\omega k}|^2}{2\sigma_n^2}} e^{-\frac{|A(m)|^2}{2\sigma_A^2}} dA(m) \\ &= \int_{A(m) \in \mathbb{C}} e^{-\frac{F}{2\sigma_A^2\sigma_n^2}} dA(m) \end{aligned}$$

where F is defined as

$$\begin{aligned} F &:= \sigma_A^2 |\mathbf{y}_k(m) - A(m)e^{j\omega k}|^2 + \sigma_n^2 |A(m)|^2 \\ &= \sigma_A^2 \left[|\mathbf{y}_k(m)|^2 - 2\Re(A(m)\mathbf{y}_k^*(m)e^{j\omega k}) \right. \\ &\quad \left. + |A(m)|^2 \right] + \sigma_n^2 |A(m)|^2 \\ &= (\sigma_A^2 + \sigma_n^2) |A(m)|^2 \\ &\quad - 2\Re \left[A(m) (\sigma_A^2 \mathbf{y}_k^*(m)e^{j\omega k}) \right] + \sigma_A^2 |\mathbf{y}_k(m)|^2 \end{aligned}$$

and $\Re(\cdot)$ ($\Im(\cdot)$) extracts the real (imaginary) part of its argument. Let $W^* := (\sigma_A^2 \mathbf{y}_k(m)^* e^{j\omega k}) / (\sigma_A^2 + \sigma_n^2)$; then

$$\begin{aligned} F &= (\sigma_A^2 + \sigma_n^2) \left[|A(m)|^2 - 2\Re(A(m)W^*) + |W|^2 \right] \\ &\quad - (\sigma_A^2 + \sigma_n^2) |W|^2 + \sigma_A^2 |\mathbf{y}_k(m)|^2 \\ &= (\sigma_A^2 + \sigma_n^2) |A(m) - W|^2 + \frac{\sigma_A^2 \sigma_n^2}{\sigma_A^2 + \sigma_n^2} |\mathbf{y}_k(m)|^2. \end{aligned}$$

We now readily see that $\mathfrak{J}_{A(m)}$ can be written as

$$\begin{aligned} \mathfrak{J}_{A(m)} &= \int_{A(m) \in \mathbb{C}} e^{-\frac{(\sigma_A^2 + \sigma_n^2) |A(m) - W|^2}{2\sigma_A^2 \sigma_n^2}} e^{-\frac{|\mathbf{y}_k(m)|^2}{2(\sigma_A^2 + \sigma_n^2)}} dA(m) \\ &= e^{-\frac{|\mathbf{y}_k(m)|^2}{2(\sigma_A^2 + \sigma_n^2)}} \int_{A(m) \in \mathbb{C}} e^{-\frac{|A(m) - W|^2}{2\frac{\sigma_A^2 \sigma_n^2}{\sigma_A^2 + \sigma_n^2}}} dA(m) \end{aligned}$$

$$\begin{aligned} &= e^{-\frac{|\mathbf{y}_k(m)|^2}{2(\sigma_A^2 + \sigma_n^2)}} \times \int_{\Re(A(m))} \int_{\Im(A(m))} e^{-\frac{(\Re(A(m)) - \Re(W))^2}{2\frac{\sigma_A^2 \sigma_n^2}{\sigma_A^2 + \sigma_n^2}}} \\ &\quad - \frac{(\Im(A(m)) - \Im(W))^2}{2\frac{\sigma_A^2 \sigma_n^2}{\sigma_A^2 + \sigma_n^2}} \\ &\quad \times e^{-\frac{(\Re(A(m)) - \Re(W))^2}{2\frac{\sigma_A^2 \sigma_n^2}{\sigma_A^2 + \sigma_n^2}}} d\Re(A(m)) d\Im(A(m)) \\ &= e^{-\frac{|\mathbf{y}_k(m)|^2}{2(\sigma_A^2 + \sigma_n^2)}} \times \left[\int_{\Re(A(m))} e^{-\frac{(\Re(A(m)) - \Re(W))^2}{2\frac{\sigma_A^2 \sigma_n^2}{\sigma_A^2 + \sigma_n^2}}} d\Re(A(m)) \right. \\ &\quad \left. \times \int_{\Im(A(m))} e^{-\frac{(\Im(A(m)) - \Im(W))^2}{2\frac{\sigma_A^2 \sigma_n^2}{\sigma_A^2 + \sigma_n^2}}} d\Im(A(m)) \right]. \end{aligned}$$

This yields

$$\begin{aligned} \mathfrak{J}_A^{(m)} &= e^{-\frac{|\mathbf{y}_k(m)|^2}{2(\sigma_A^2 + \sigma_n^2)}} \left[\sqrt{\frac{\pi}{\frac{\sigma_A^2 \sigma_n^2}{2(\sigma_A^2 + \sigma_n^2)}}} \right] \times \left[\sqrt{\frac{\pi}{\frac{\sigma_A^2 \sigma_n^2}{2(\sigma_A^2 + \sigma_n^2)}}} \right] \\ &= 2\pi \frac{\sigma_A^2 \sigma_n^2}{\sigma_A^2 + \sigma_n^2} e^{-\frac{|\mathbf{y}_k(m)|^2}{2(\sigma_A^2 + \sigma_n^2)}}. \end{aligned}$$

D_2 can now be written as

$$\begin{aligned} D_2 &= \frac{h}{(2\pi)^{(2L+1)} \sigma_A^{2L} \sigma_n^{2L}} \\ &\quad \times \int_{\omega \in [-\pi, \pi]} \prod_{m=1}^L \left[2\pi \frac{\sigma_A^2 \sigma_n^2}{\sigma_A^2 + \sigma_n^2} e^{-\frac{|\mathbf{y}_k(m)|^2}{2(\sigma_A^2 + \sigma_n^2)}} \right] d\omega \\ &= \frac{h}{(2\pi (\sigma_A^2 + \sigma_n^2))^L} e^{-\frac{\sum_{m=1}^L |\mathbf{y}_k(m)|^2}{2(\sigma_A^2 + \sigma_n^2)}}, \end{aligned}$$

$$\begin{aligned} D_1 &= \frac{1-h}{(2\pi\sigma_n^2)^L} \int_{\omega \in [-\pi, \pi]} \int_{A^{(1)} \in \mathbb{C}} \cdots \int_{A^{(L)} \in \mathbb{C}} \prod_{m=1}^L \left[e^{-\frac{|\mathbf{y}_k(m) - A^{(m)}e^{j\omega k}|^2}{2\sigma_n^2}} \right] \\ &\quad \times \left[\delta(\omega - \omega_{n,k-1}) \prod_{m=1}^L \delta(A^{(m)} - A_{n,k-1}^{(m)}) \right] dA^{(1)} \cdots dA^{(L)} d\omega \\ &= \frac{1-h}{(2\pi\sigma_n^2)^L} e^{-\frac{\sum_{m=1}^L |\mathbf{y}_k(m) - A_{n,k-1}^{(m)}e^{j\omega_{n,k-1} k}|^2}{2\sigma_n^2}}, \end{aligned}$$

and

$$\begin{aligned} D_2 &= \int_{\omega \in [-\pi, \pi]} \int_{A^{(1)} \in \mathbb{C}} \cdots \int_{A^{(L)} \in \mathbb{C}} \frac{1}{(2\pi\sigma_n^2)^L} \frac{1}{(2\pi\sigma_A^2)^L} \frac{h}{2\pi} \\ &\quad \times e^{-\frac{\sum_{m=1}^L |\mathbf{y}_k(m) - A^{(m)}e^{j\omega k}|^2}{2\sigma_n^2}} e^{-\frac{\sum_{m=1}^L |A^{(m)}|^2}{2\sigma_A^2}} dA^{(1)} \cdots dA^{(L)} d\omega \\ &= \frac{h}{(2\pi)^{(2L+1)} \sigma_A^{2L} \sigma_n^{2L}} \\ &\quad \times \int_{\omega \in [-\pi, \pi]} \prod_{m=1}^L \left[\int_{A^{(m)} \in \mathbb{C}} e^{-\frac{|\mathbf{y}_k(m) - A^{(m)}e^{j\omega k}|^2}{2\sigma_n^2}} e^{-\frac{|A^{(m)}|^2}{2\sigma_A^2}} dA^{(m)} \right] d\omega. \end{aligned}$$

$$\begin{aligned}
p_0(\mathbf{x}_k | \mathbf{x}_{n,k-1}, \mathbf{y}_k) &:= \delta(\omega_k - \omega_{n,k-1}) \prod_{m=1}^L \delta\left(A_k^{(m)} - A_{n,k-1}^{(m)}\right) \\
p_1(\mathbf{x}_k | \mathbf{x}_{n,k-1}, \mathbf{y}_k) &:= \frac{\frac{1}{(2\pi\sigma_n^2)^L} \frac{1}{(2\pi\sigma_A^2)^L} \frac{1}{2\pi} e^{-\sum_{m=1}^L \frac{|y_k^{(m)} - A_k^{(m)} e^{j\omega_k}|^2}{2\sigma_n^2}} e^{-\sum_{m=1}^L \frac{|A_k^{(m)}|^2}{2\sigma_A^2}}}{\frac{1}{(2\pi)^L} \frac{1}{(\sigma_n^2 + \sigma_A^2)^L} e^{-\sum_{m=1}^L \frac{|y_k^{(m)}|^2}{2(\sigma_n^2 + \sigma_A^2)}}}, \\
\tilde{h} &:= h \frac{\frac{1}{(2\pi)^L} \frac{1}{(\sigma_n^2 + \sigma_A^2)^L} e^{-\sum_{m=1}^L \frac{|y_k^{(m)}|^2}{2(\sigma_n^2 + \sigma_A^2)}}}{D(\mathbf{y}_k, \mathbf{x}_{n,k-1})}.
\end{aligned}$$

and

$$\begin{aligned}
D(\mathbf{y}_k, \mathbf{x}_{n,k-1}) &= \frac{1 - \tilde{h}}{(2\pi\sigma_n^2)^L} \\
&\times e^{-\sum_{m=1}^L \frac{|y_k^{(m)} - A_{n,k-1}^{(m)} e^{j\omega_{n,k-1} k}|^2}{2\sigma_n^2}} \\
&+ \frac{\tilde{h}}{(2\pi(\sigma_n^2 + \sigma_A^2))^L} e^{-\sum_{m=1}^L \frac{|y_k^{(m)}|^2}{2(\sigma_n^2 + \sigma_A^2)}}.
\end{aligned}$$

The weight update is given by

$$w_{n,k} \propto w_{n,k-1} p(\mathbf{y}_k | \mathbf{x}_{n,k-1}) = w_{n,k-1} D(\mathbf{y}_k, \mathbf{x}_{n,k-1})$$

followed by normalization to 1.

As in the $L = 2$ case, $p(\mathbf{x}_k | \mathbf{x}_{n,k-1}, \mathbf{y}_k)$ can be written as a mixture of two pdfs

$$\begin{aligned}
p(\mathbf{x}_k | \mathbf{x}_{n,k-1}, \mathbf{y}_k) &= (1 - \tilde{h}) p_0(\mathbf{x}_k | \mathbf{x}_{n,k-1}, \mathbf{y}_k) \\
&+ \tilde{h} p_1(\mathbf{x}_k | \mathbf{x}_{n,k-1}, \mathbf{y}_k)
\end{aligned}$$

where the constituent pdfs and \tilde{h} are given at the top of the page. It follows that with probability $1 - \tilde{h}$ we simply copy the previous particle, else we draw a particle from $p_1(\mathbf{x}_k | \mathbf{x}_{n,k-1}, \mathbf{y}_k)$. This can be accomplished via Rao-Blackwellization, as done for $L = 2$ in the text.

REFERENCES

- [1] M. S. Arulampalam, S. Maskell, N. Gordon, and T. Clapp, "A tutorial on particle filters for nonlinear/non-Gaussian Bayesian tracking," *IEEE Trans. Signal Process.*, vol. 50, no. 2, pp. 174–188, Feb. 2002.
- [2] L. Aydin and A. Polydoros, "Hop-timing estimation for FH signals using a coarsely channelized receiver," *IEEE Trans. Commun.*, vol. 44, no. 4, pp. 516–526, Apr. 1996.
- [3] S. Barbarossa and A. Scaglione, "Parameter estimation of spread spectrum frequency-hopping signals using time-frequency distributions," in *Proc. Int. Workshop Signal Process. Adv. Wireless Commun. (SPAWC'97)*, Apr. 1997, pp. 213–216.
- [4] P. Djuric, J. H. Kotecha, J. Zhang, Y. Huang, T. Ghirmai, M. Bugallo, and J. Miguez, "Particle filtering," *IEEE Signal Process. Mag.*, pp. 19–38, Sep. 2003.
- [5] A. Doucet, S. J. Godsill, and C. Andrieu, "On sequential Monte Carlo sampling methods for Bayesian filtering," *Statist. Comput.*, vol. 10, no. 3, pp. 197–208, 2000.

- [6] A. Doucet, N. Gordon, and V. Krishnamurthy, "Particle filters for state estimation of jump Markov linear systems," *IEEE Trans. Signal Process.*, vol. 49, no. 3, pp. 613–624, Mar. 2001.
- [7] A. Doucet and X. Wang, "Monte Carlo methods for signal processing: A review in the statistical signal processing context," *IEEE Signal Process. Mag.*, vol. 22, no. 6, pp. 152–170, Nov. 2005.
- [8] N. J. Gordon, D. J. Salmond, and A. F. M. Smith, "Novel approach to nonlinear/non-Gaussian Bayesian state estimation," *IEE Proc.-F*, vol. 140, no. 2, pp. 107–113, 1993.
- [9] X. Liu, N. D. Sidiropoulos, and A. Swami, "Blind high resolution localization and tracking of multiple frequency Hopped signals," *IEEE Trans. Signal Process.*, vol. 50, no. 4, pp. 889–901, Apr. 2002.
- [10] X. Liu, N. D. Sidiropoulos, and A. Swami, "Joint hop timing and frequency estimation for collision resolution in frequency hopped networks," *IEEE Trans. Wireless Commun.*, vol. 4, no. 6, pp. 3063–3074, Nov. 2005.
- [11] T. Schon, F. Gustafsson, and P.-J. Nordlund, "Marginalized particle filters for mixed linear/nonlinear state-space models," *IEEE Trans. on Signal Process.*, vol. 53, no. 7, pp. 2279–2289, Jul. 2005.
- [12] N. D. Sidiropoulos, A. Swami, and A. Valyrakis, "Tracking a frequency hopped signal using particle filtering," in *Proc. IEEE ICASSP 2006*, Toulouse, France, May 14–19, 2006.
- [13] M. K. Simon, U. Cheng, L. Aydin, A. Polydoros, and B. K. Levitt, "Hop timing estimation for noncoherent frequency-hopped M-FSK intercept receivers," *IEEE Trans. Commun.*, vol. 43, no. 2/3/4, pp. 1144–1154, Feb./Mar./Apr. 1995.
- [14] E. Tsakonas, N. D. Sidiropoulos, and A. Swami, "Time-frequency analysis using particle filtering: Closed-form optimal importance function and sampling procedure for a single time-varying harmonic," in *Proc. Nonlin. Statist. Signal Process. Workshop: Classical, Unscented, and Particle Filtering Methods*, Cambridge, U.K., Sep. 13–15, 2006, Corpus Christi College.
- [15] E. Tsakonas, N. D. Sidiropoulos, and A. Swami, "Optimal particle filters for tracking a time-varying harmonic or chirp signal," *IEEE Trans. Signal Process.*, vol. 56, no. 10, pp. 4598–4610, Oct. 2008.
- [16] A. Valyrakis, N. D. Sidiropoulos, and A. Swami, "Multichannel particle filtering for tracking a frequency hopped signal," in *Proc. IEEE CAMSAP 2007*, St. Thomas, U.S. Virgin Islands, Dec. 12–14, 2007.



Alexandros S. Valyrakis received the B.Sc. degree in telecommunications and electronic engineering from the Greek Air Force Academy, in 2003, and the M.Sc. degree in electronic and computer engineering from the Technical University of Crete (TUC), Greece, in 2007.

He is currently an officer in the Greek Air Force, and continues graduate studies with the Department of Production Engineering and Management, TUC. His research interests are in signal processing for communications and radar.



Efthimios E. Tsakonas received the Diploma in electronic and computer engineering from the Technical University of Crete (TUC), Greece, in 2008.

He is currently a visiting researcher with the TUC. He is planning to join KTH, Sweden, to pursue the Ph.D. degree in fall 2009. His current research interests are in particle filtering and convex approximation theory and algorithms, with applications in the broad area of signal processing and communications.



Nicholas D. Sidiropoulos (F'09) received the Diploma degree from the Aristotelian University of Thessaloniki, Greece, and the M.Sc. and Ph.D. degrees from the University of Maryland at College Park (UMCP), in 1988, 1990, and 1992, respectively, all in electrical engineering.

He has been a Postdoctoral Fellow (1994–1995) and Research Scientist (1996–1997) with the Institute for Systems Research, UMCP, and has held positions as Assistant Professor, Department of Electrical Engineering, University of Virginia-Charlottesville (1997–1999), and Associate Professor, Department of Electrical and Computer Engineering, University of Minnesota—Minneapolis (2000–2002). Since 2002, he has been a Professor with the Department of Electronic and Computer Engineering, Technical University of Crete, Chania-Crete, Greece, and an Adjunct Professor with the University of Minnesota. His current research interests are primarily in signal processing for communications, convex approximation of NP-hard problems, cross-layer resource allocation for wireless networks, and multiway analysis.

Prof. Sidiropoulos received the U.S. NSF CAREER Award (1998), the IEEE Signal Processing Society Best Paper Award (in 2001 and in 2007), and is

currently a Distinguished Lecturer of the IEEE SP Society (2008–2009). He has served as a member (2000–2004), Vice-Chair (2005–2006), and Chair (2007–2008) of the Signal Processing for Communications and Networking Technical Committee (SPCOM-TC), and as a member of the Sensor Array and Multichannel Technical Committee (SAM-TC) of the IEEE SP Society (2004–2009). He has served as an Associate Editor for the IEEE TRANSACTIONS ON SIGNAL PROCESSING (2000–2006) and IEEE SIGNAL PROCESSING LETTERS (2000–2002), and currently serves on the editorial board of the IEEE *Signal Processing Magazine*.



Ananthram Swami (F'08) received the B.Tech. degree from Indian Institute of Technology (IIT), Bombay; the M.S. degree from Rice University, Houston, TX, and the Ph.D. degree from the University of Southern California (USC), Los Angeles, all in electrical engineering.

He has held positions with Unocal Corporation, USC, CS-3 and Malgudi Systems. He was a Statistical Consultant to the California Lottery, developed a Matlab-based toolbox for non-Gaussian signal processing, and has held visiting faculty positions at INP,

Toulouse, France. He is with the U.S. Army Research Laboratory (ARL) where his work is in the broad area of signal processing, wireless communications, sensor and mobile *ad hoc* networks.

Dr. Swami is a member of the IEEE Signal Processing Society's (SPS) Technical Committee (TC) on Sensor Array and Multichannel systems, and serves on the Senior Editorial Board of the IEEE JOURNAL ON SELECTED TOPICS IN SIGNAL PROCESSING. He was a tutorial speaker on "Networking Cognitive Radios for Dynamic Spectrum Access" at ICASSP 2008, DySpan 2008, and MILCOM 2008, and coeditor of the book *Wireless Sensor Networks: Signal Processing & Communications Perspectives* (New York: Wiley, 2007). He is an ARL Fellow.